

ENCLOSURE FOR
RESEARCH INFORMATION LETTER

on

EVALUATION OF METHOD FOR PREDICTING
RESIDUAL STRESSES IN GIRTH-BUTT WELDS

SUMMARY

A finite element model for predicting residual stresses due to girth-butt welds in pressure vessels and pipes was developed at Battelle's Columbus Laboratories. The residual stress model for girth-butt welds was verified for welds in pipes ranging from 2 to 30 passes. The model also accurately predicts residual deformations. Comparisons of results from the model with data indicate that the model can be extended to accurately represent weld repairs in pressure vessels. A summary of the accomplishments directed at developing and evaluating the model is given in the following:

- A critical review of the literature was made to evaluate analytical techniques for developing the model and identify residual stress data to be used in verifying the models.
- Experimental studies of two girth-butt welded pipes were conducted to provide temperature data and residual stress data for verifying the models. Data obtained from these experiments include residual stresses, temperatures during welding, strains during welding, and residual deflections of the welded pipe.
- Two experiments on girth-butt welded pipes were identified from the literature as test cases for the model.
- A description of the pipes for which data was obtained from the experimental study and through the literature is given in the following. All pipes are 304 stainless steel.

Pipe Identification	Outside Pipe Diameter (in.)	Pipe Wall Thickness (in.)	Number of Weld Passes
BCL Model No. 2	12.75	.180	2
BCL Model No. 3	12.75	.375	6
Argonne Pipe	4.50	.337	7
General Electric Pipe	28.00	1.300	30

- A model for predicting residual stresses in girth-butt welds of pressure vessels and pipes was developed. The model consists of two parts; a temperature model and a stress analysis model.
- The temperature model was developed through modification of a model described in the literature review. Good comparisons between temperature data and computations by the model were obtained for each pass of the two-pass and six-pass welds. The temperature model includes heat input, pipe thickness, location of weld pass, thermal properties of the pipe, torch speed, efficiency of the weld process, and time dependent effects.
- A finite element model for girth-butt welds was developed. The model includes temperature dependent material properties, elastic-plastic stress strain effects, the effects of changing geometry of the pipe as it is welded, and linear elastic unloading from an elastic-plastic state of stress. The weld geometry and number of weld passes are also represented by the model.
- Results of the residual stress model showed good agreement with residual stress data in the hoop and axial directions on the insides and outsides of the four pipes described above.
- Preliminary results were obtained using the residual stress model to represent a weld repair of the HSST Intermediate Vessel V-8. While the model needs further development before it can adequately represent the weld repair geometry, qualitative agreement between residual stress data and results of the model were obtained.

- Thus, an analytical model for predicting residual stresses in girth-butt welds has been developed and verified by comparison with experimentally obtained data for four pipes. It was demonstrated that with further development, the model can be applicable to other weld configurations such as weld repair of pressure vessels.

The following sections describe the model's capabilities and limitations, the girth-butt welds used for the validation study, and comparisons of predicted residual stress distributions and those obtained from the welds.

MODEL CAPABILITIES AND LIMITATIONS

Figure 1 shows an illustration of a girth-butt weld. The residual stress model is comprised of two parts: a heat flow model and a stress analysis model. The heat flow model provides transient temperature distributions which are the input for the finite element stress analysis model. The stress analysis model gives the magnitudes and distributions of the residual stresses including variations through the pipe thickness. The model represents important parameters of the welding process. These are contained in the following list:

- Size and number of weld passes
- Elastic-plastic temperature dependent response of the pipe and weld materials
- Heat flow analysis
- Geometry of pipe and weld groove
- Heat input of weld process
- Speed of weld torch
- Time dependent transient aspects of the weld process
- Interpass temperatures
- Mechanical end restraints of the pipes.

The model for pipe welds is limited to axisymmetric representations and hence does not contain variations in stresses around the circumference

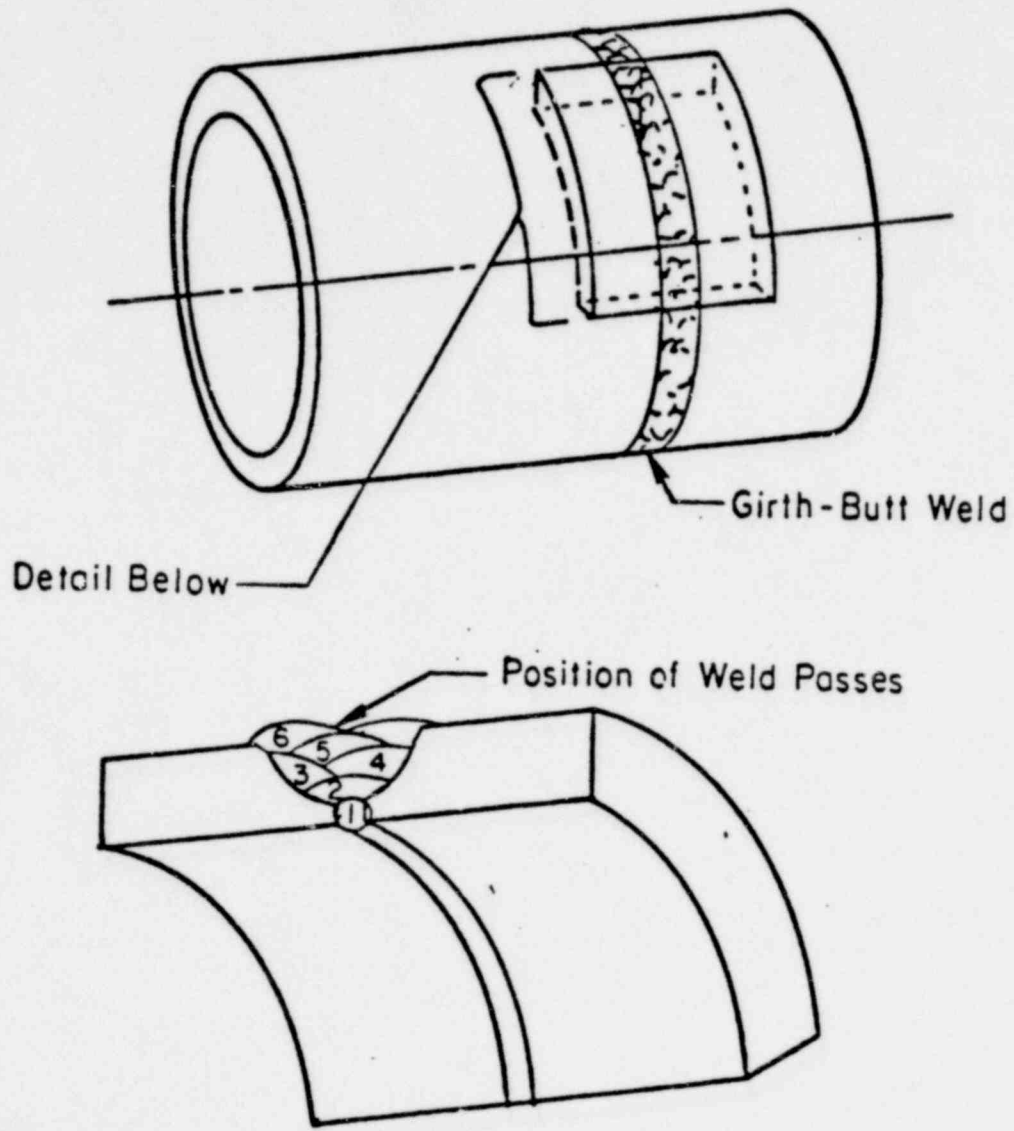


FIGURE 1. ILLUSTRATION OF GIRTH-BUTT WELD

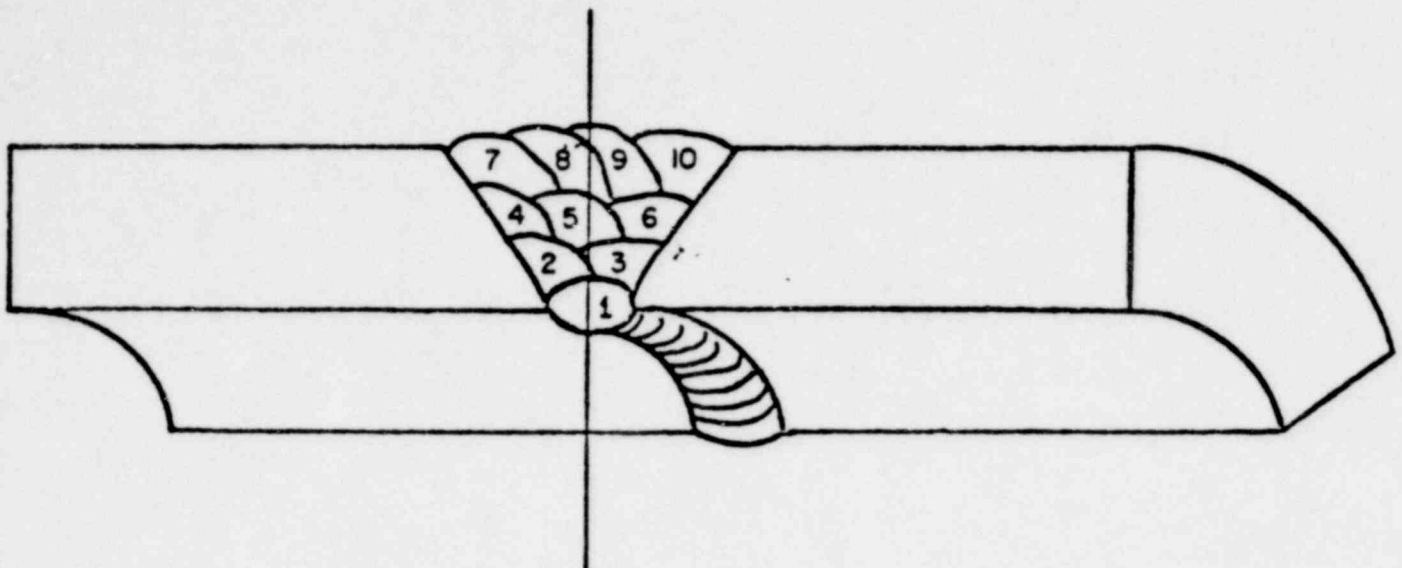
of the pipe. This is however not a serious limitation because circumferential variations in residual stresses can be explained with results of the model. Furthermore, the weld repair model does contain circumferential variations in the residual stress distribution.

In addition to the axisymmetric simplification of the girth-butt weld program, several additional simplifications were examined. One which was included primarily because of the reduction in computer costs, was treating the girth-butt weld procedure as being symmetric about the plane which is perpendicular to the axis of the pipe and passes through the center of the weld bead. This resulted in a computer cost savings of approximately 50 percent. Closely related to this simplification and in part resulting from it, was the modeling of a sequence of weld passes as a layer rather than as individual weld passes. The savings resulting from this simplification is dependent on the pipe size and number of passes, with the savings being greater for pipes with more passes. The method of modeling a general multipass girth-butt weld under these two assumptions is shown in Figure 2.

DETAILS OF THE MODELS FOR HEAT FLOW
AND RESIDUAL STRESSES

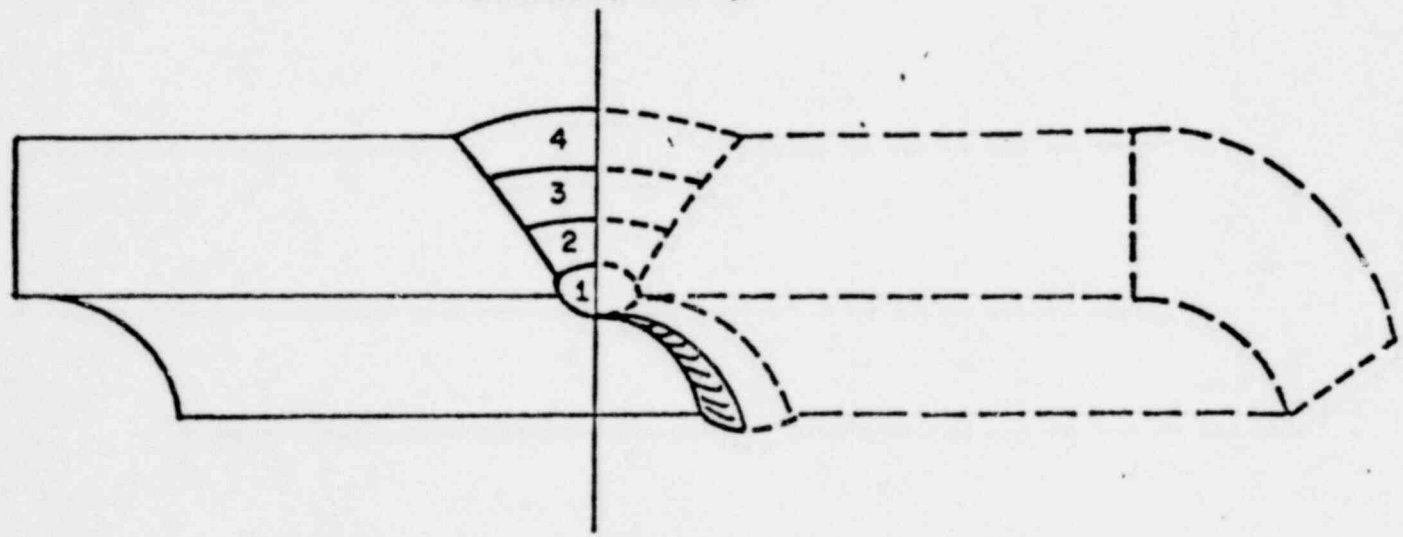
The focus of this study is on the magnitude and distribution of residual stresses. However, a representative model for predicting residual stresses requires accurate information about the temperatures due to the welding processes. Temperature information can come from thermal measurements, models for predicting temperatures, or a combination of these two sources. The approach taken here was to develop a temperature analysis procedure and verify the capability of the model to predict temperature distributions by comparing results with the data. The following sections describe the temperature analysis.

Weld Centerline



a. Weld Cross Section Geometry with Ten Passes

Line of Symmetry



b. Model of Weld Cross Section Geometry Using Four Layers

FIGURE 2. COMPARISON OF ACTUAL AND MODEL WELD CROSS SECTIONS

Temperature Analysis During Welding

The technique for modeling the temperature distributions is based on the distribution of temperatures around a moving point-heat source in an infinite solid. The temperature due to this moving heat source is given by the following equation.

$$T(r, \zeta) = T_0 + \frac{q}{4\pi K} \frac{\left[\exp\left(-\frac{V\zeta}{2a}\right) \right] \exp\left(-\frac{Vr}{2a}\right)}{r}, \quad (1)$$

where

- T = Temperature
- T₀ = Ambient temperature
- q = Rate of heat input
- K = Thermal conductivity
- V = Heat source velocity
- ζ = X-distance from heat source
- r = Distance from heat source
- c = Heat capacity
- a = K/c.

Equation (1) is identical to that presented by Rosenthal [23]*. Time does not explicitly appear as a variable in Equation (1) because, although the temperature distribution is variable with respect to a stationary point in a solid, it is unchanging with respect to the heat source since steady-state conditions are assumed to be present. However, time does appear implicitly in Equation (1) since

$$\zeta = X_0 - Vt, \quad (2)$$

where X₀ is the distance between the stationary point and the heat source when t = 0.

The numerical technique approximates the temperature rise due to the moving source in a finite thickness plate by superposing a series of heat sources. One heat source, located on the pipe, is the actual welding source. Other heat

* Numbers in brackets denote references in the Bibliography and References Section.

sources are placed outside of the pipe to eliminate the heat transfer through the inside pipe surface and the outside surface. The actual pipe temperature distribution is obtained by superposing at least 28 temperature sources.

The superposition of heat sources, each described by Equation (1), is used to compute time dependent temperatures for the heat source moving along the circumference of a pipe of specified thickness. The pipe is represented as a plate with length equal to the circumference of the pipe.

The solution for the point heat source given by Equation (1) is valid only for physical properties independent of temperature. The solution also applies only outside of the fused zone of the weld. The time temperature curve for all points inside the fused zone are generated by

$$T_f = T_o + \frac{q}{4\pi K} \cdot \frac{1}{\xi} \quad (2)$$

where T_o , q , K , and (ξ) are identical to the variables defined for Equation (1).

The multipass welding of a pipe is modeled by the following procedure. Temperatures will be calculated for the root pass by applying and locating the main heat source at the centroid of the root pass. For the second pass, temperatures are calculated by locating the heat source at the center of the second pass. The total temperature will be obtained by adding the temperatures to an experimentally determined ambient temperature for the second pass.

Numerical Results for Temperatures

The temperature model was used to generate temperature-time profiles for comparison with the thermocouple data. These comparisons are shown in Figures 3 and 4. Figure 3 displays comparisons for the gas-tungsten arc root pass and Figure 4 shows comparisons for the second or gas-metal arc pass. The smallest time value in each figure corresponds to the time at which the thermocouple nearest the weld centerline reached its maximum temperature. The difference between the results of the temperature model and the experimental data was less than 9 percent for the first pass and less than 17 percent for the second pass.

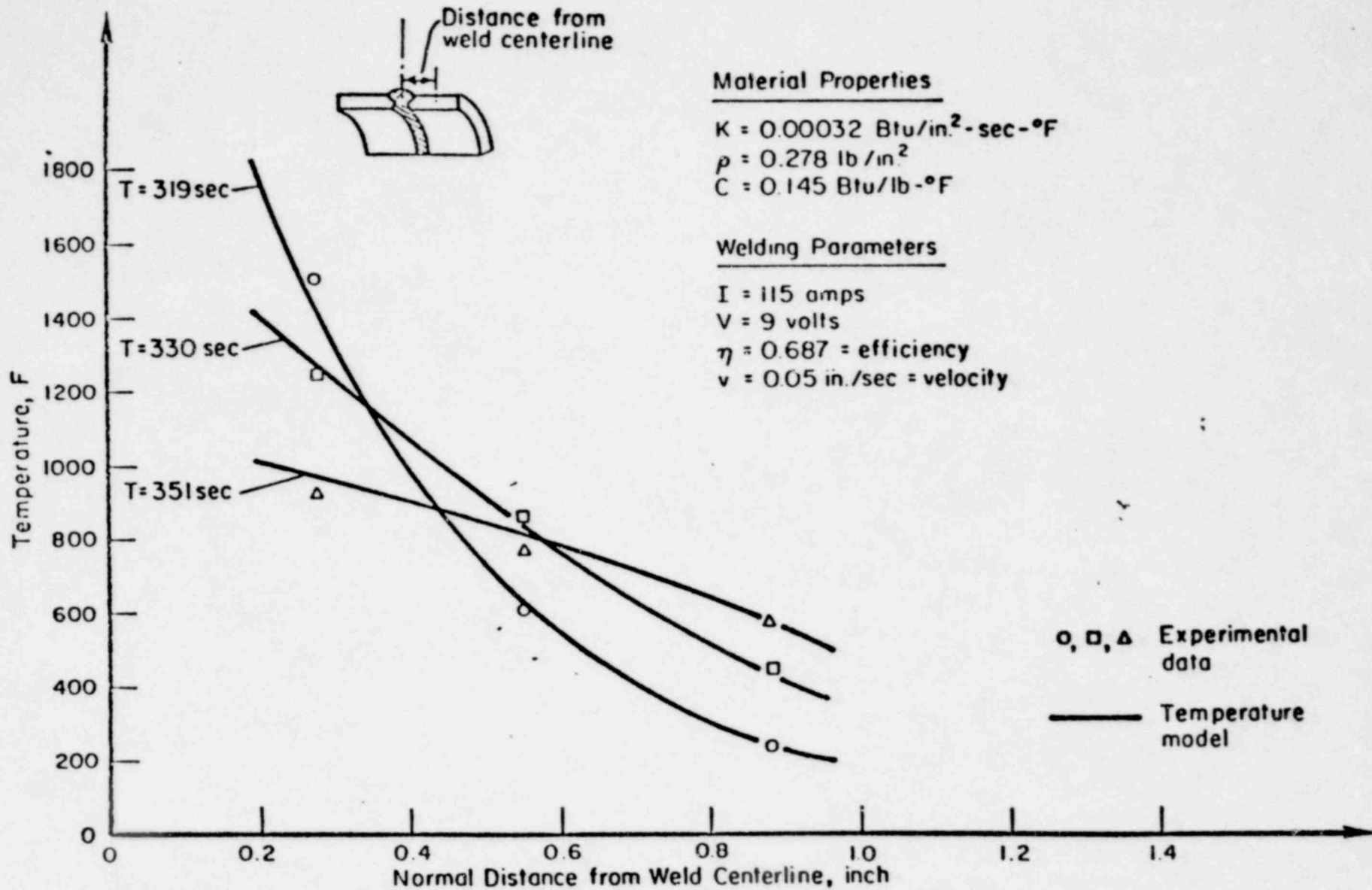


FIGURE 3. CALCULATED TEMPERATURE CURVES AND EXPERIMENTAL DATA FOR THE ROOT PASS

1568 143

13-85

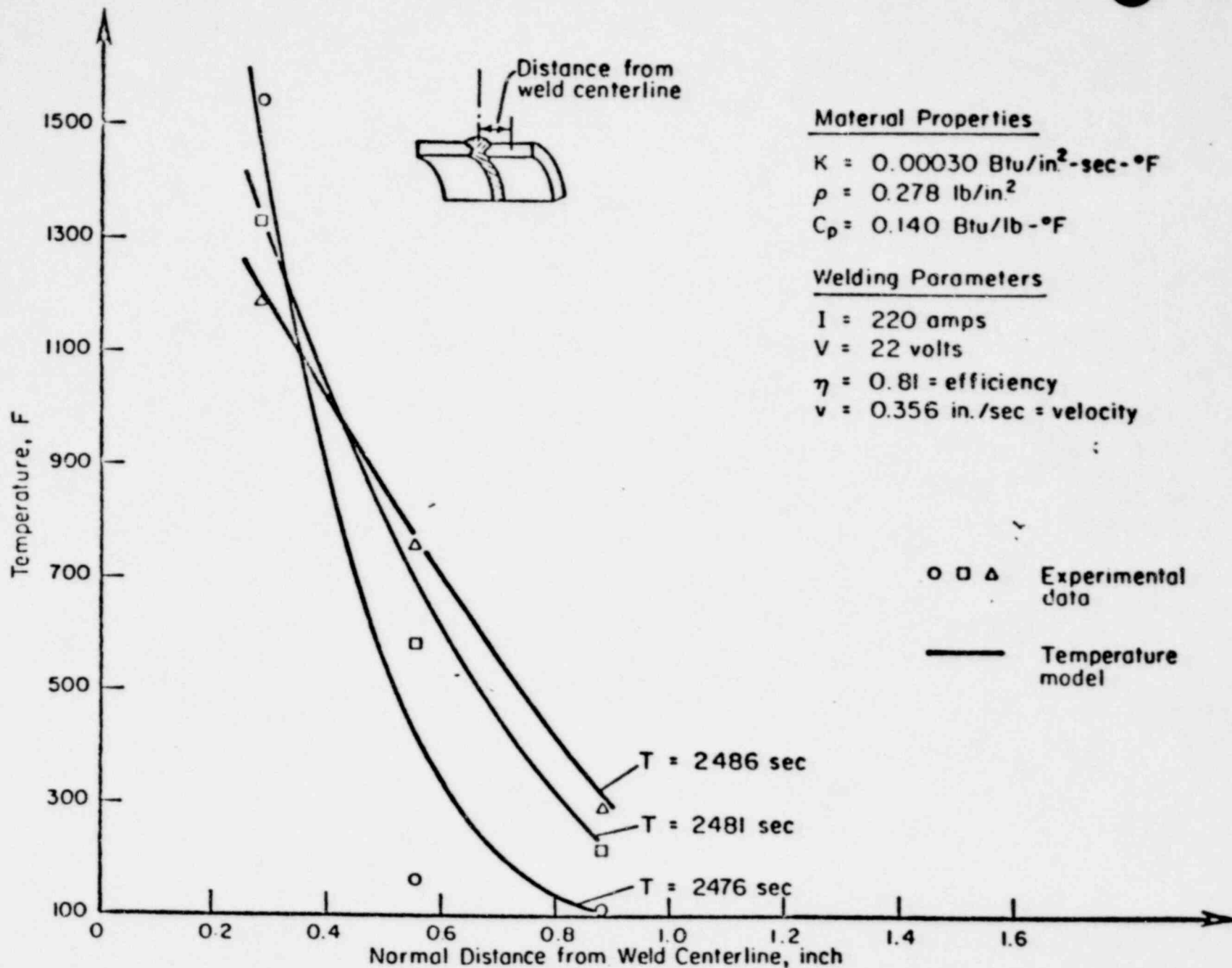


FIGURE 4. CALCULATED TEMPERATURE CURVES AND EXPERIMENTAL DATA FOR PASS 2

1568 144

13-810

Finite Element Model for Residual Stresses

Figure 5 shows an axisymmetric, finite element representation for a portion of a 323.85-mm diameter pipe welded by two passes. The cross section of the pipe and the weld groove are represented by finite elements. Each element is assigned to one of three zones. Zone 1 represents the weld material that is being deposited. Since the model consists of finite elements representing the entire weld region, a zone with essentially zero stiffness is assigned to elements in the areas which are to be filled by subsequent passes. This artificial zone is represented by Zone 2. Zone 3 consists of a portion of the pipe and the previously deposited weld material that experience a transient temperature increase as a result of the welding.

During each weld pass, thermal deformations are calculated from temperature distributions determined by the thermal model. These residual deformations at the end of each pass are added to determine an updated configuration of the model before analyzing the next pass. Therefore, a large deformation, elastic-plastic problem is broken into a series of incrementally linear problems. The analysis procedure also includes temperature-dependent material properties which are varied for each pass. Material properties of 304 stainless steel used in this study are shown in Figure 6 as a function of temperature.

The analysis procedure is also based on several assumptions given as follows. Melting or dilution of the pipe material is not included in the analysis. The mass of the weld and base materials are also neglected. The shape of each weld pass is obtained from photographs of the experimental weld-pass cross sections.

An axisymmetric finite element computer program with the capability to model elastic unloading from an elastic-plastic state of stress was used to represent the pipe. The need to include unloading of this type arises because high stresses that occur near the weld are reduced as the weld and base metal cool. Thus, finite elements in this area must permit a reduction in stress while maintaining a residual plastic strain. In the computer program, an unloading criterion is automatically checked at each element. The criterion is a reduction of equivalent stress between two consecutive load increments. If an element meets this criterion, then during the next load increment that element is assigned a stiffness based on the elastic material properties.

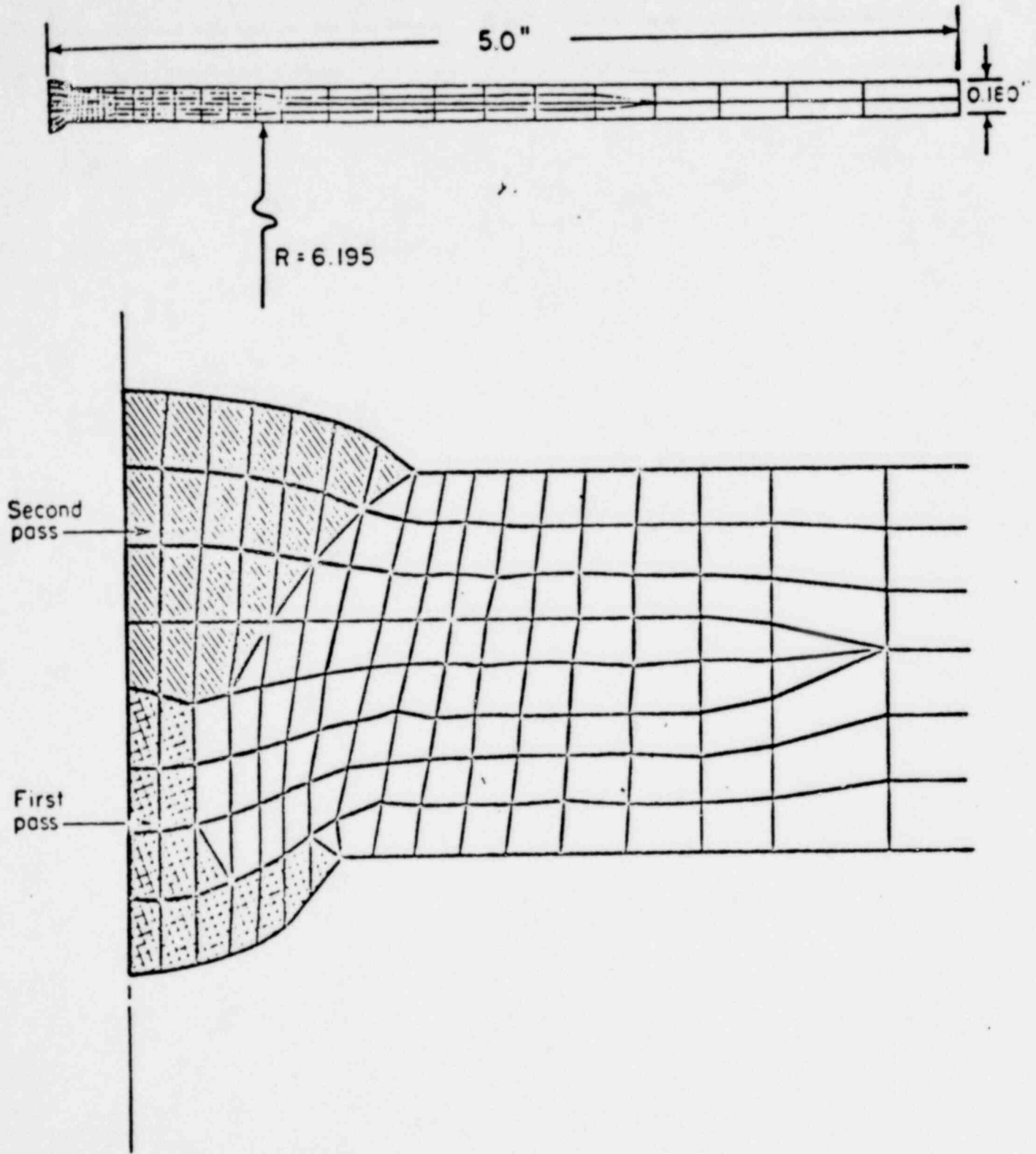


FIGURE 5. FINITE ELEMENT MODEL FOR TWO-PASS WELD

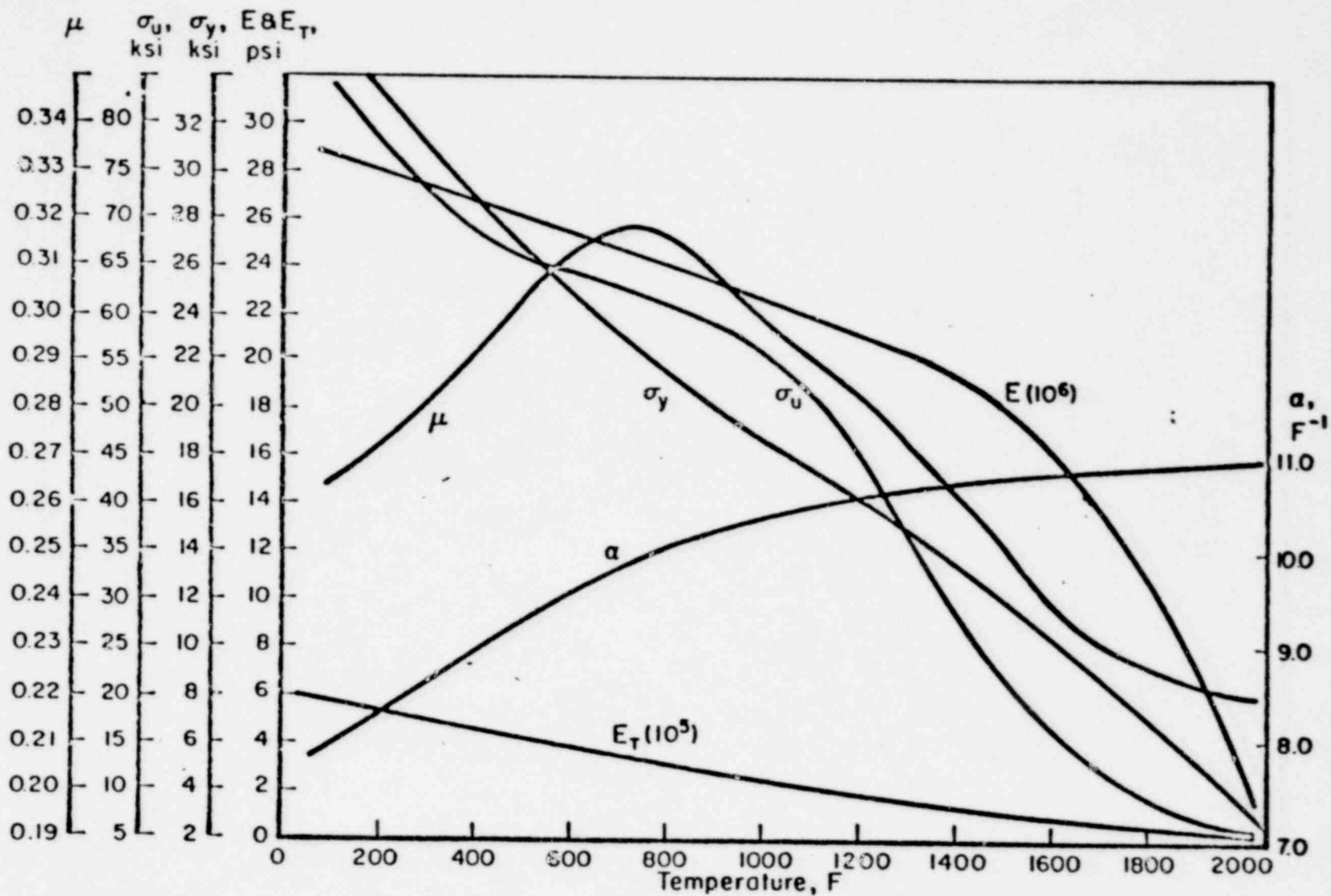


FIGURE 6. 304 STAINLESS STEEL TEMPERATURE DEPENDENT PROPERTIES USED FOR FINITE ELEMENT STRESS ANALYSIS

1568 147

13-89

Numerical Results

A numerical test case for unloading was conducted to demonstrate that the stress-strain behavior of the elements could follow the input stress-strain curve. A stainless steel with a yield stress of 220.0 MPa, a thermal expansion of 17.6×10^{-6} mm/mm/C an initial modulus of 186×10^3 MPa, and a modulus of 20.7×10^3 above the yield stress was selected for the test case. A thermal load of 66 C was applied to a 25.4 mm x 76.2 mm steel plate of unit thickness in four load increments, and reduced to 33 C in four increments. All sides of the plate were rigidly clamped. The stress-strain behavior of a typical element during this loading history is shown in Figure 7 along with the theoretical curve for the stress-strain behavior.

Computed values for the residual stress at the inner and outer surfaces of the two-pass welded pipe are compared to the experimentally obtained values in Figures 8 and 9, respectively. Qualitatively, the experimental points and the analytical curves agree well. As can be seen from these figures, the quantitative agreement at the inner surface is better than that for the outer surface, and the hoop stresses generally show better agreement than the axial stresses at both surfaces. The figures show that some oscillation in the calculated hoop stresses occurs in the hoop stresses at the outer surface. This is due to the discontinuity of modulus which results at the interface between the weld material and pipe material. This behavior is more noticeable at the outer surface because during the placement of the outer pass, the root pass and the pipe material act as one material, and oscillations in the stresses due to the prior application of the inner pass are reduced by the plasticity resulting from the outer pass.

Deformations of the welded pipes were also compared with measured values as a means of verifying the model. A comparison of predicted values and measurements for the two pass weld are shown in Figure 10. This figure shows good agreement between the predictions on the model and the data. The figure also shows that the results are not overly sensitive to logical variations in representing the temperature distributions. This is a desirable trait for the model.

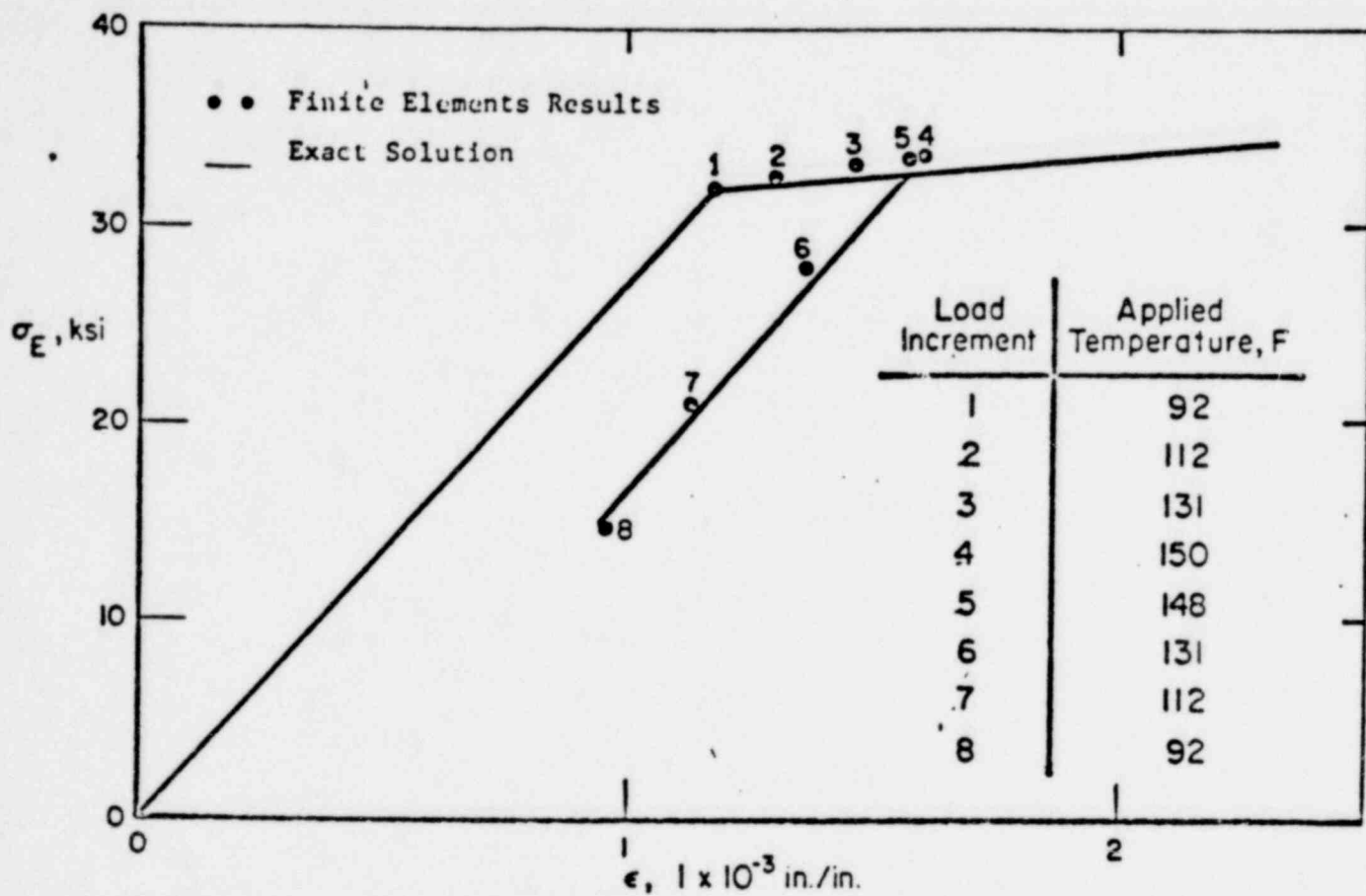


FIGURE 7. STRESS-STRAIN RESPONSE OF ZERO STRAINED ELEMENT FOR PLASTIC LOADING AND LINEAR-ELASTIC UNLOADING

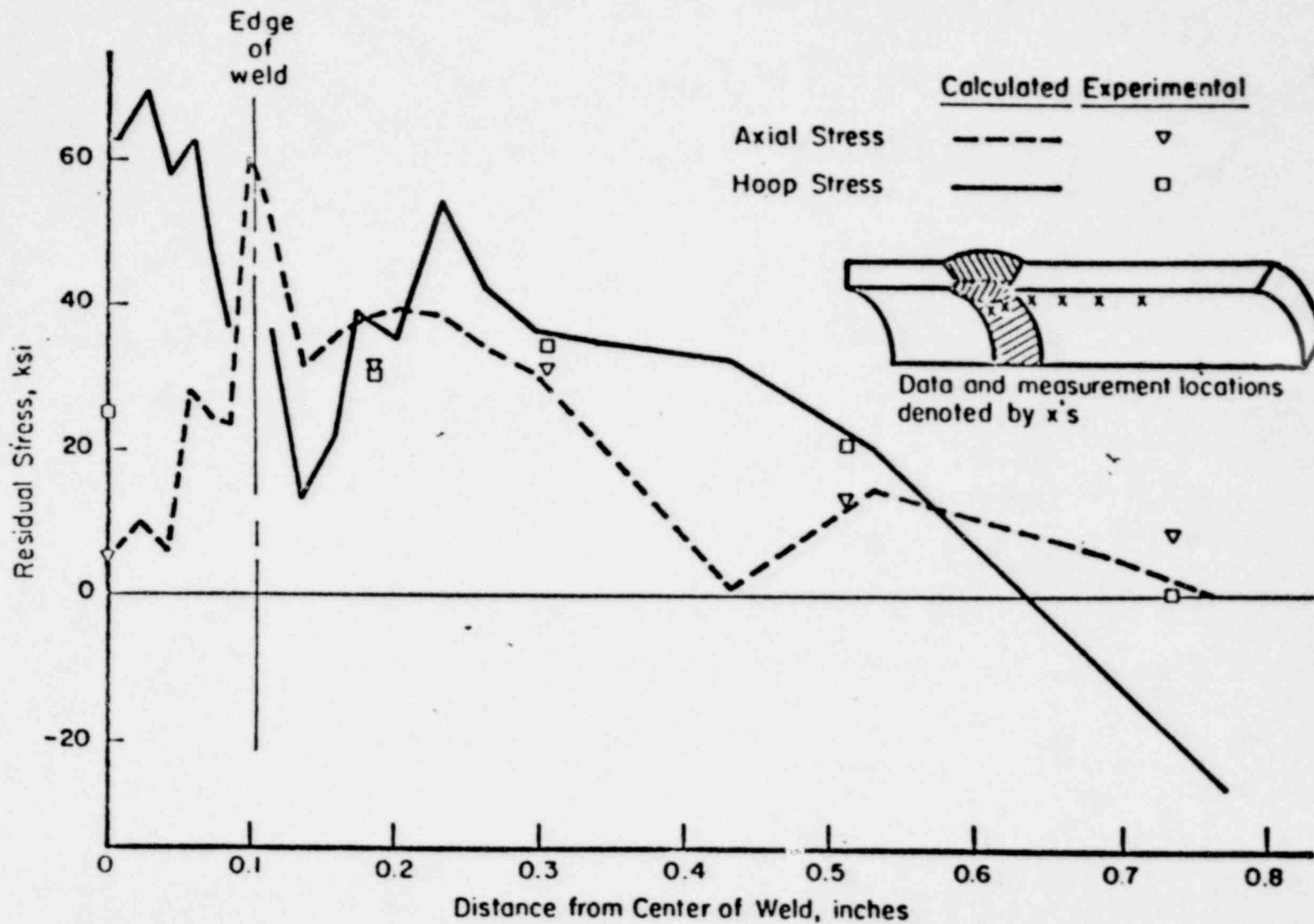


FIGURE 8. COMPARISON OF CALCULATED AND EXPERIMENTALLY OBTAINED RESIDUAL STRESSES AT THE INNER SURFACE FOR TWO-PASS WELD

1568 150

13-92

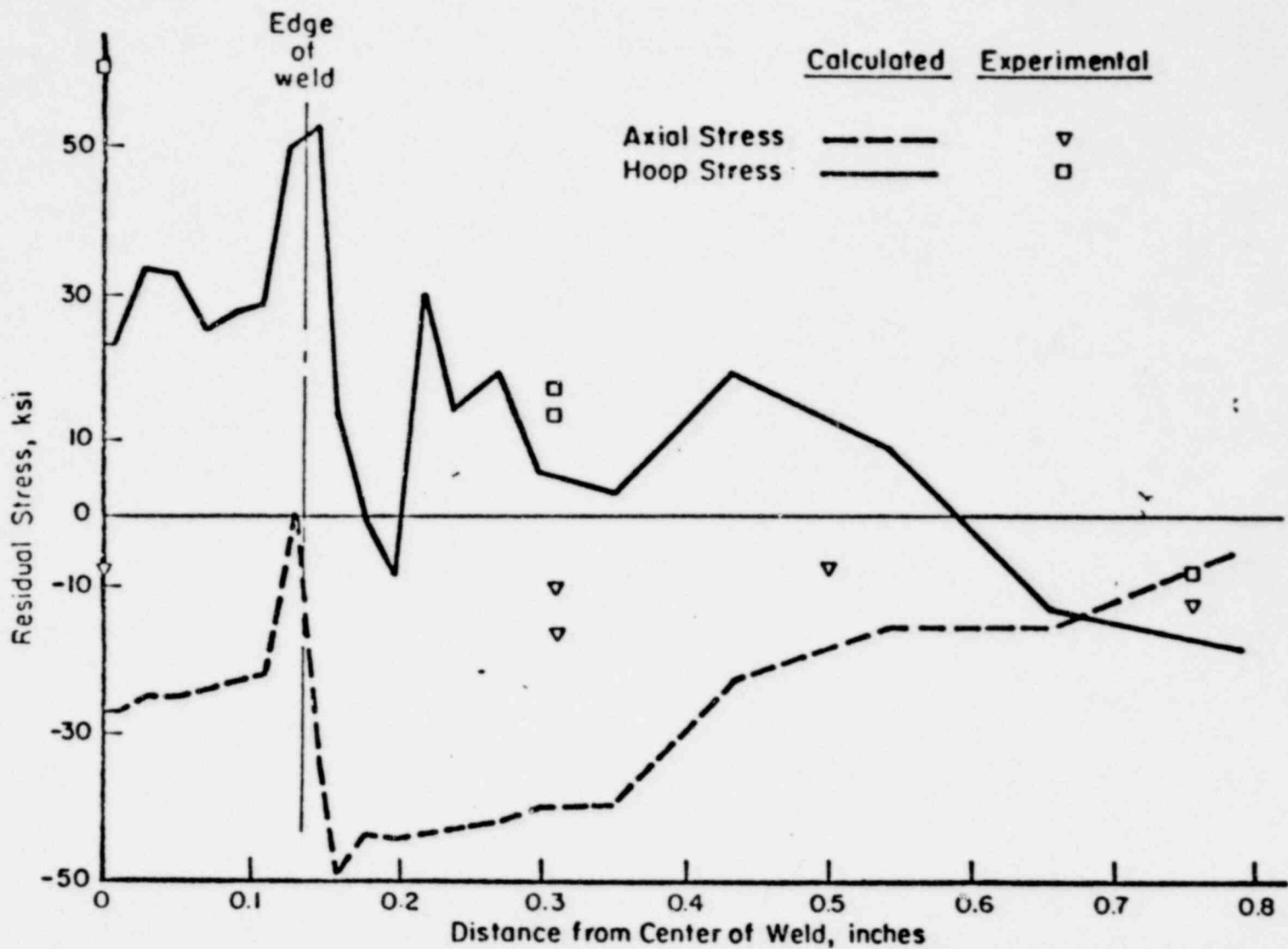


FIGURE 9. COMPARISON OF CALCULATED AND EXPERIMENTALLY OBTAINED RESIDUAL STRESSES AT THE OUTER SURFACE FOR TWO-PASS WELD

1568 151

13-93

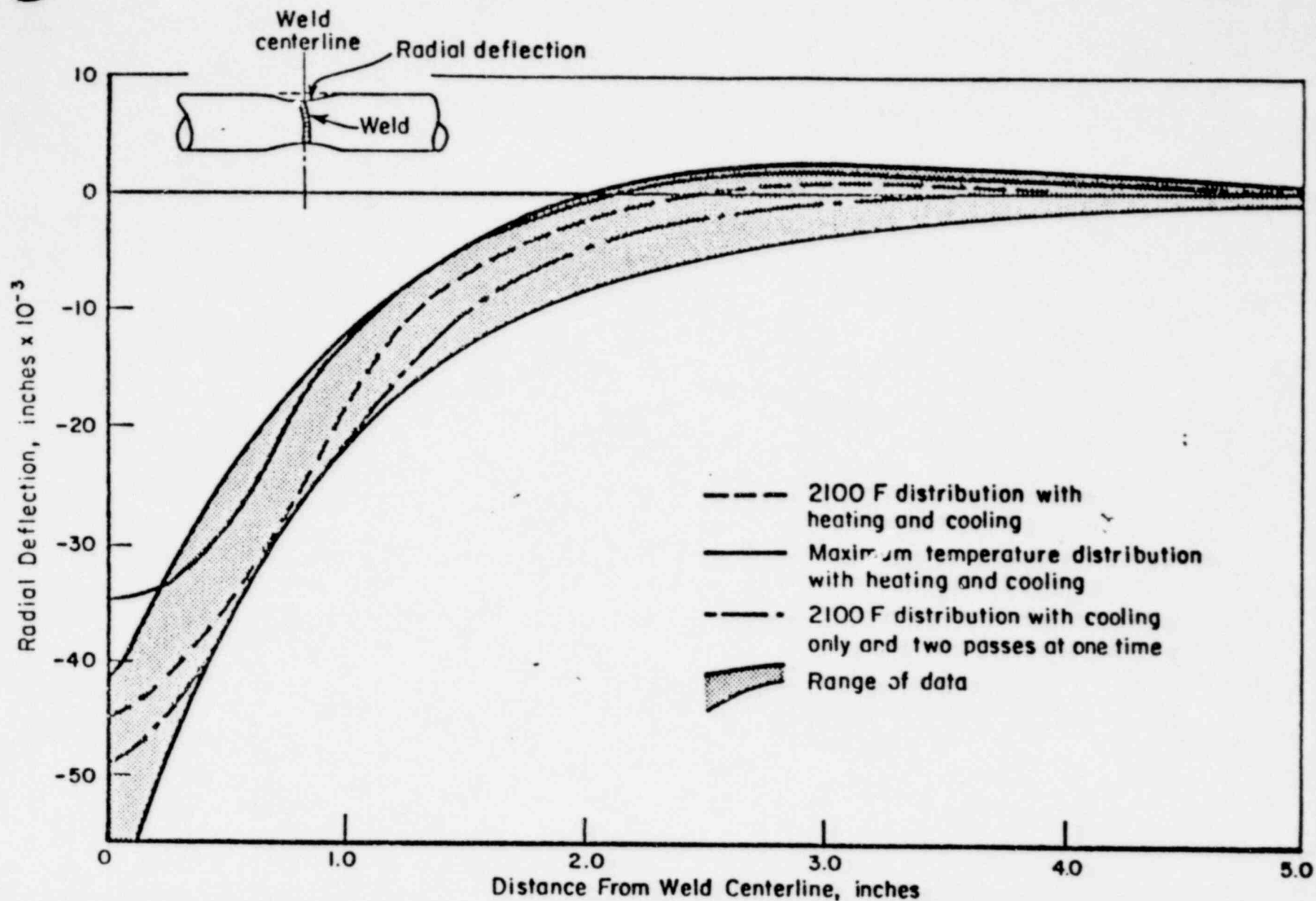


FIGURE 10. COMPARISON OF RESIDUAL DEFLECTION FOR THREE ALTERNATIVE METHODS OF REPRESENTING THE THERMAL LOADING FOR A TWO-PASS WELD

1568 152

1394

13-95

Modeling Argonne National Laboratory (ANL)
Experiment, Seven-Pass Weld

The data for this girth-butt welded pipe was obtained from measurements taken by ANL based on References [24] and [25]. The weldment is denoted by W 27A and was selected because of the relatively small pipe diameter. This pipe is Type 304 stainless steel with an outer diameter of 4.5-inches and a thickness of 0.337-inch. The cross section is shown in Figure 11.

The finite element grid generated for the seven-pass pipe is shown in Figure 12. The model has 314 elements and 350 nodes. The material was 304 stainless steel with the assumed temperature dependent properties shown in Figure 6. Figure 13 shows a comparison of the calculated and experimentally measured maximum temperature profiles.

Residual Stress Calculations

Figure 14 shows a comparison of experimentally determined stresses and values computed from the model for the inside surface of the ANL seven-pass welded pipe. The bars on this figure indicate the effect of taking data at different angular positions about the pipe circumference. The effect of nonsymmetric behavior about the weld centerline is indicated by the right and left symbols. Again, the side of the pipe on which the last pass was applied showed the largest experimentally measured stresses. The results indicate that the concept of spreading the heat input over the entire weld layer appears to be an effective representation.

Modeling General Electric Company
Experiment, Thirty-Pass Weld

This girth-butt welded pipe was fabricated by GE and selected because of the relatively large number of weld passes. The pipe material is Type 304 stainless steel with an outer diameter of 28 inches and a thickness of 1.3 inch. The cross-sectional geometry of the thirty-pass weld was obtained from Figure 15 which was obtained from the GE report describing the experiment, Reference [26].

13-96

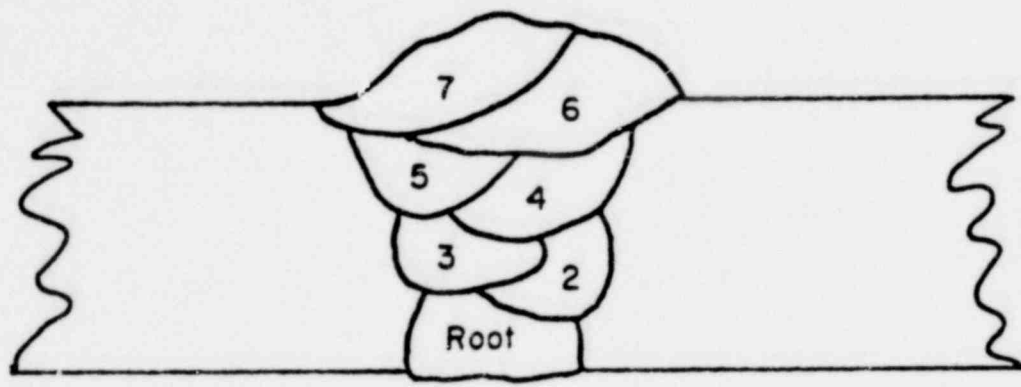


FIGURE 11. CROSS SECTION OF SEVEN-PASS ANL EXPERIMENTAL GIRTH-BUTT WELD W 27A

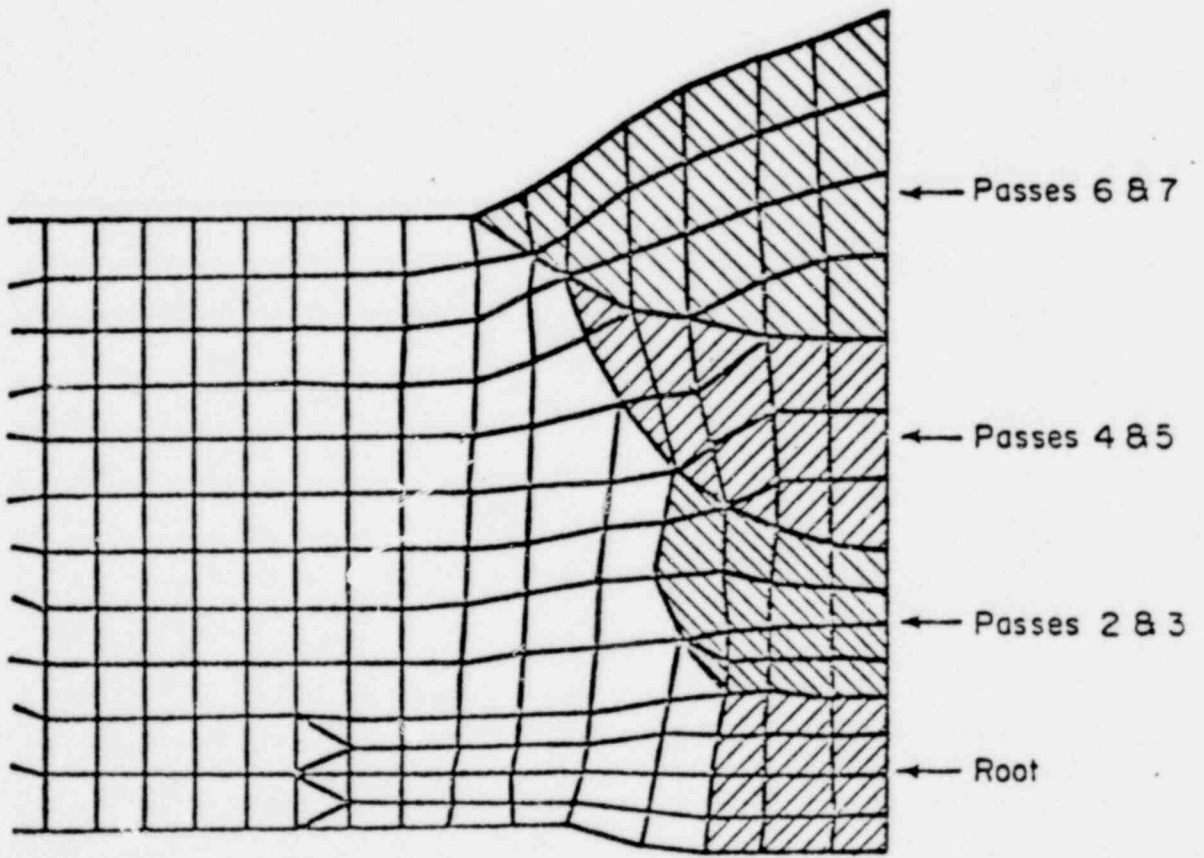
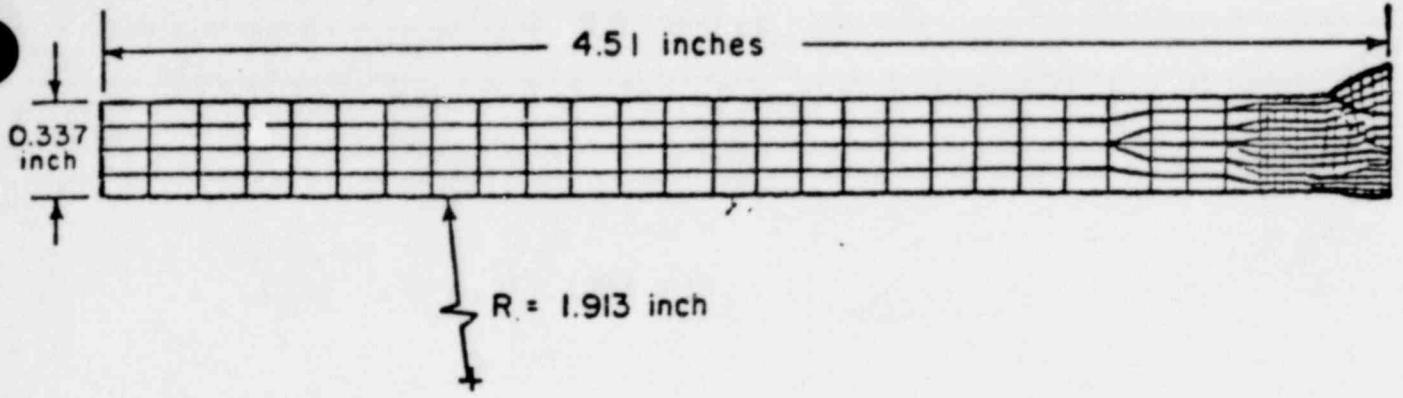


FIGURE 12. SEVEN-PASS FINITE ELEMENT MODEL FOR ANL EXPERIMENT W 27A

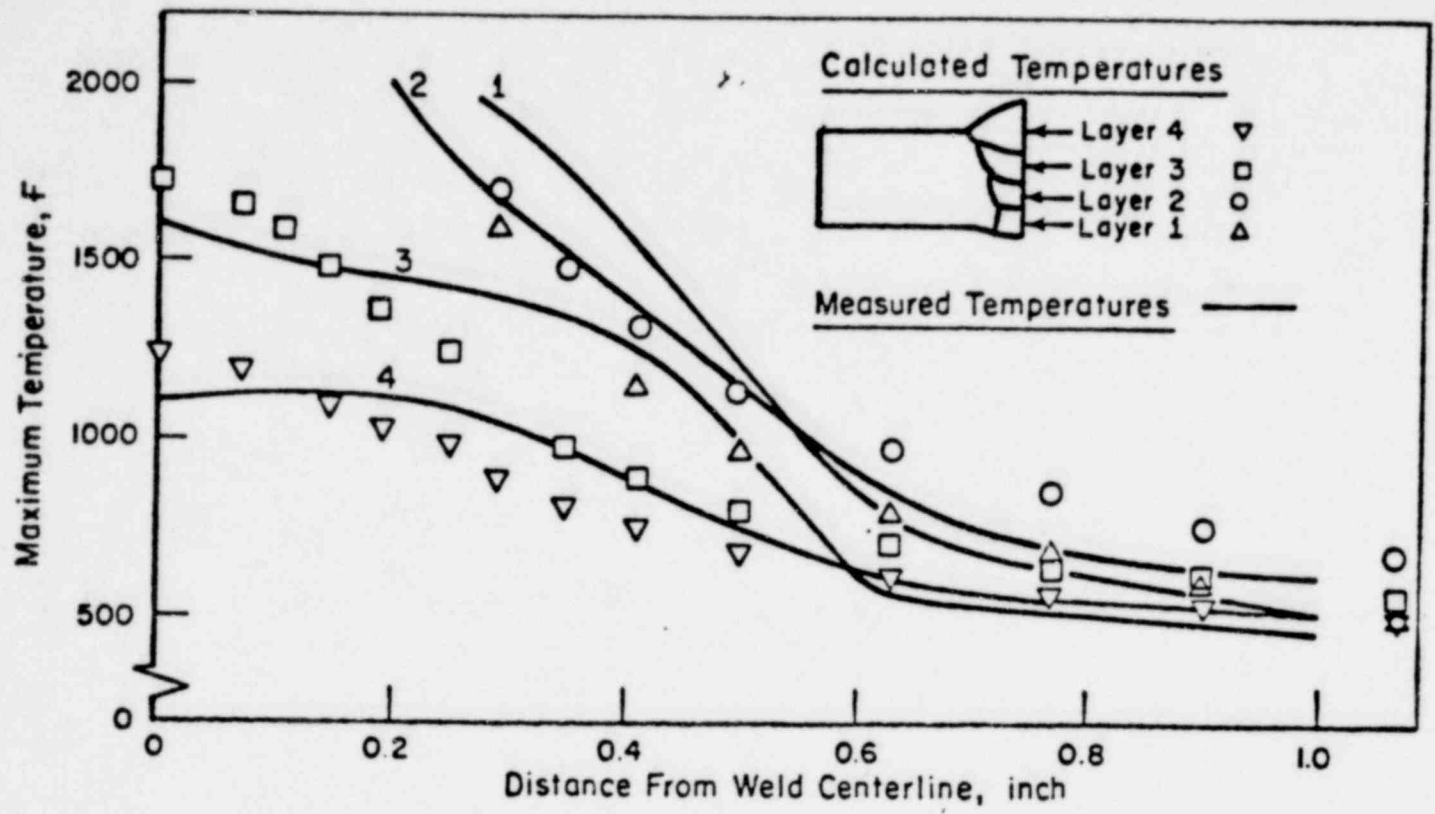


FIGURE 13. COMPARISON OF MEASURED AND CALCULATED MAXIMUM TEMPERATURE PROFILES ALONG INSIDE SURFACE FOR SEVEN-PASS ANL WELD W 27A

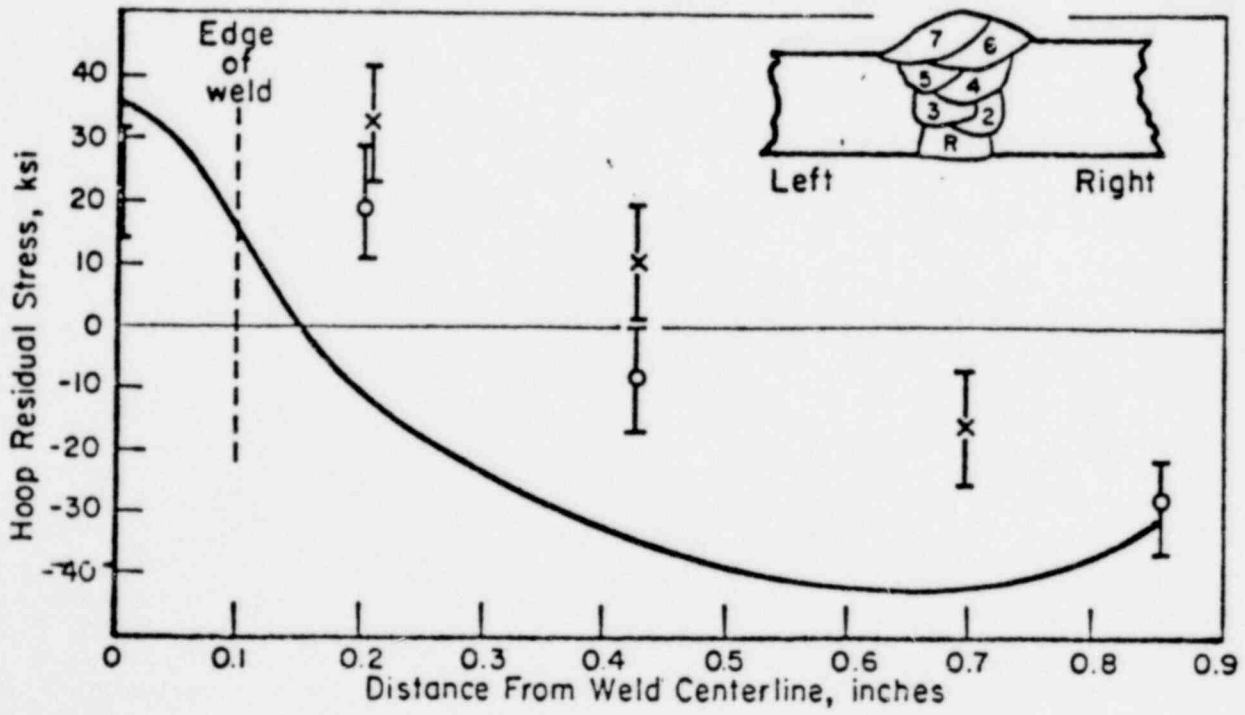
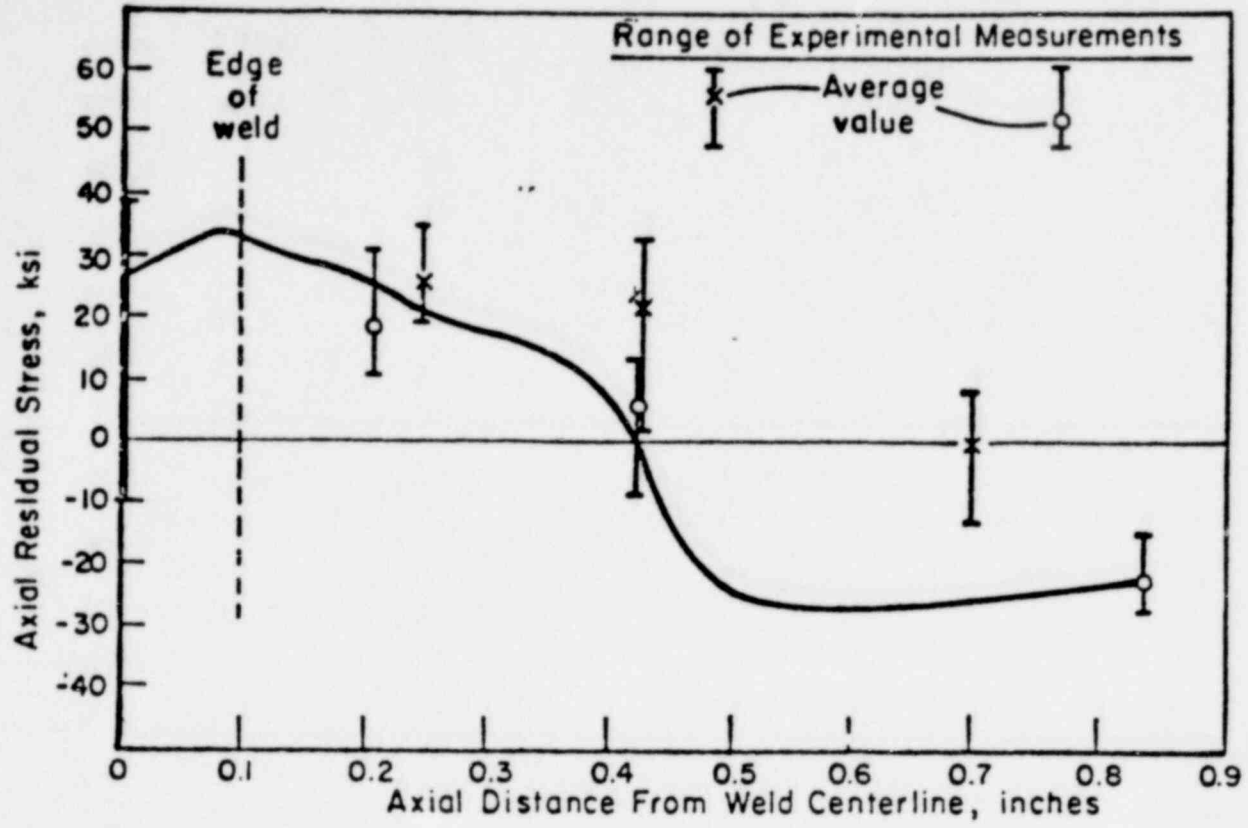


FIGURE 14. COMPARISON OF CALCULATED AND EXPERIMENTAL DETERMINED RESIDUAL STRESSES FOR THE INNER SURFACE OF SEVEN-PASS ANL EXPERIMENT W 27A

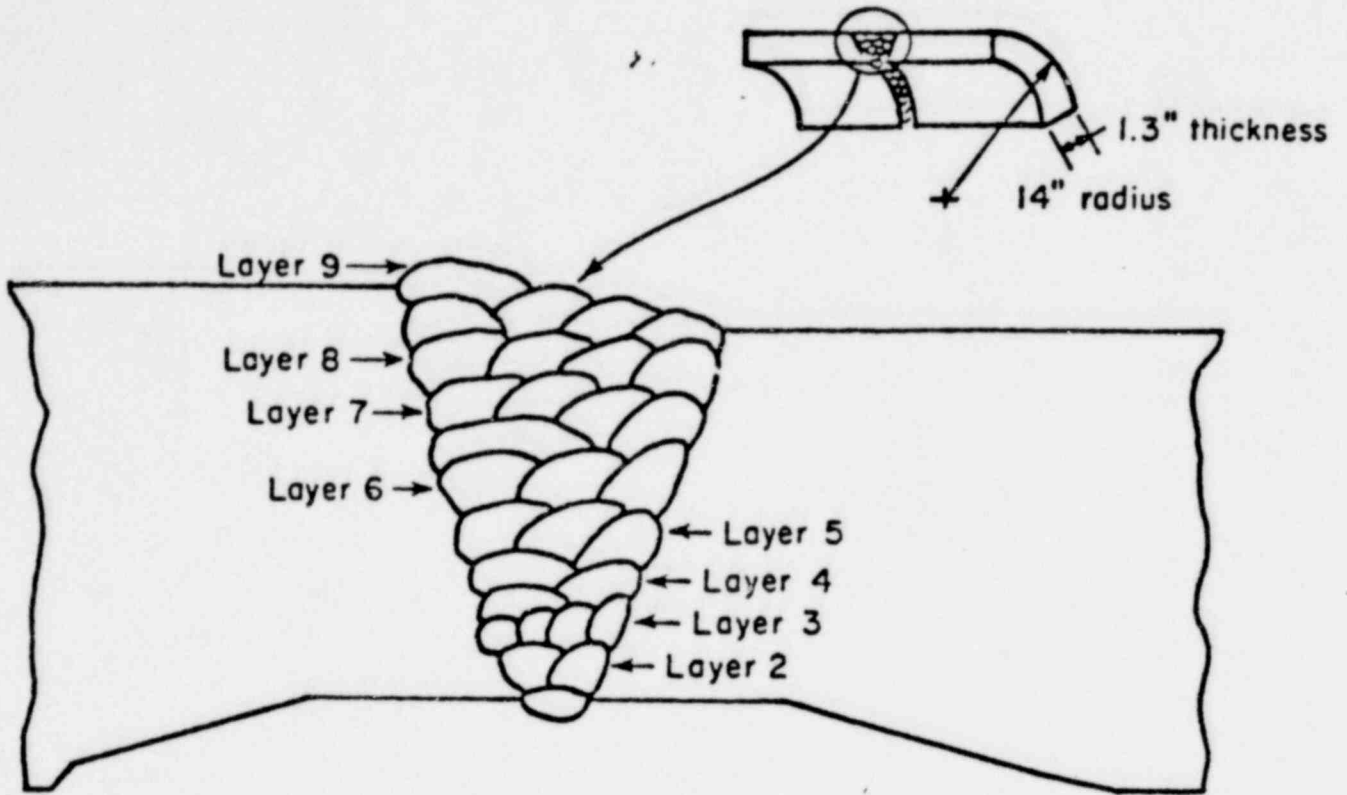


FIGURE 15. CROSS SECTION OF THIRTY-PASS GE EXPERIMENTAL GIRTH-BUTT WELD

13-101

The finite element grid for the thirty-pass pipe is shown in Figure 16. The model has 214 elements and 248 nodes. The material properties used with this model are shown in Figure 6.

The computed residual stresses for the inside surface of the thirty-pass model are compared with experimental measurements in Figure 17. The bars on this figure indicate the effect of taking measurements at different angular locations around the pipe circumference. Though experimental measurements were made on both sides of the weld centerline, data points from both sides generally fell within the same range.

The calculated stresses in both the axial and hoop directions agree quite well with the data. The axial stress sign reversal agrees with the experimental values better than for the seven-pass pipes.

One aspect of the modeling of pipes with large numbers of passes, that was briefly addressed during the study of the thirty-pass pipe, is the possibility of grouping layers of passes in the analysis procedure. At this time, not enough studies have been done to fully answer the question of how many passes can be represented by one layer in the model. However, results indicate there is merit to the modeling concept of using a layer that contains one row of weld passes.

Preliminary Application of the Residual Stress Model to a Weld Repair of a Pressure Vessel

The residual stress model described here has many potential applications to welds of pressure vessels and pipes. One such application is to understanding the residual stresses resulting from a weld repair of a pressure vessel. It is emphasized that the model, in its present form, would require some extensions before accurately representing several aspects of the problem. Nonetheless, it is of value to apply the model to this problem with the intent of obtaining qualitative results. The following contains a description of the vessel, the weld repair cavity, and the model. A comparison of residual stress data and results obtained from the model is also presented.

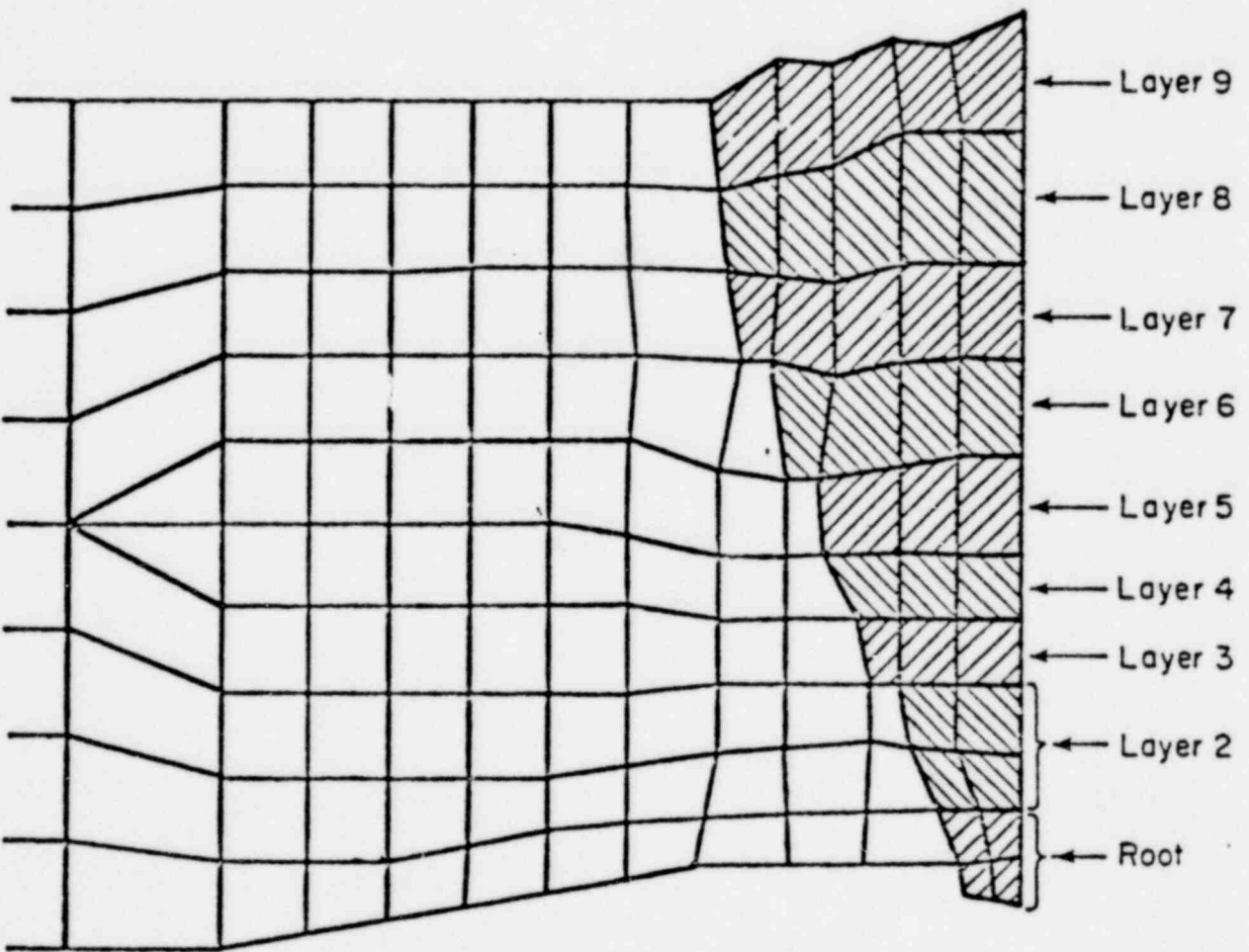
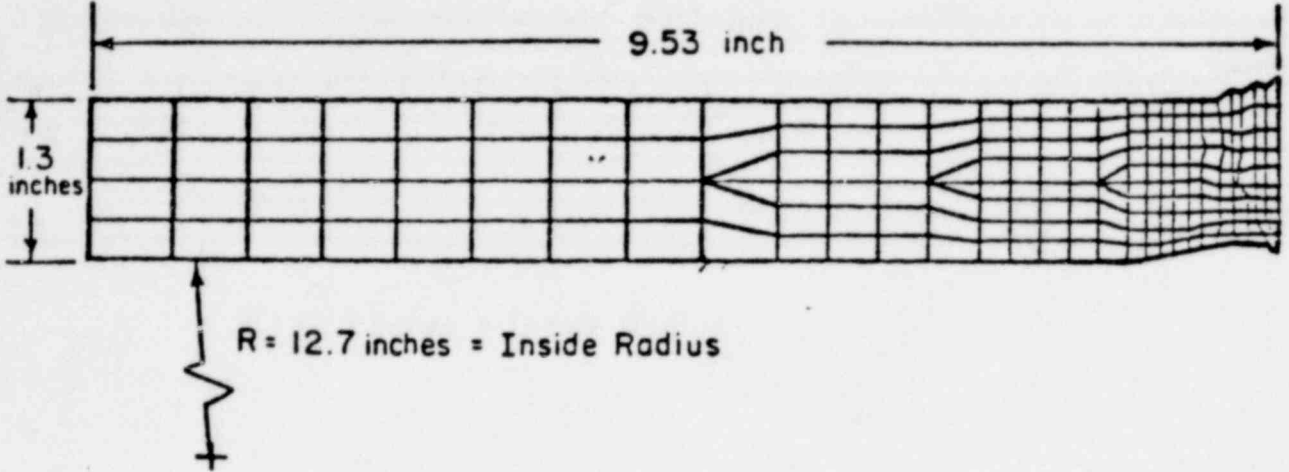


FIGURE 16. FINITE ELEMENT MODEL FOR THIRTY-PASS GE EXPERIMENTAL GIRTH-BUTT WELD

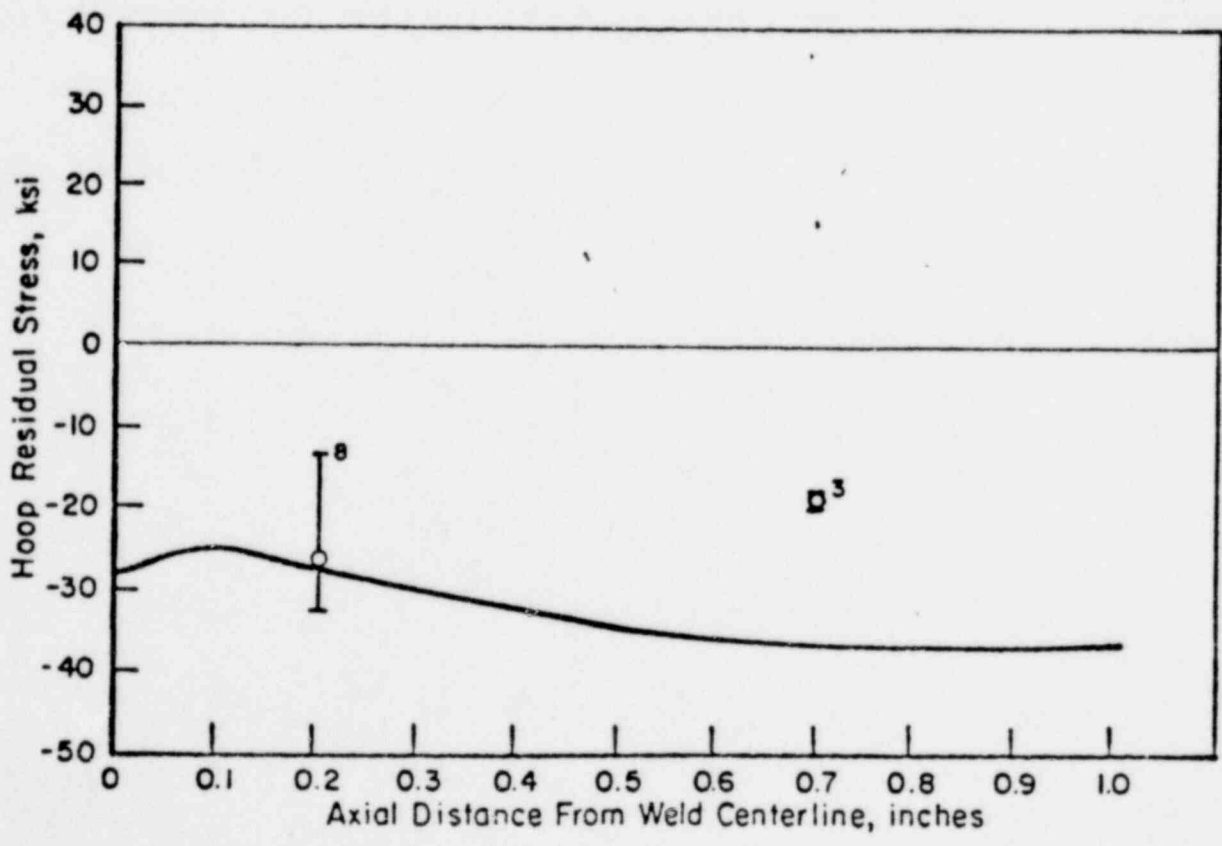
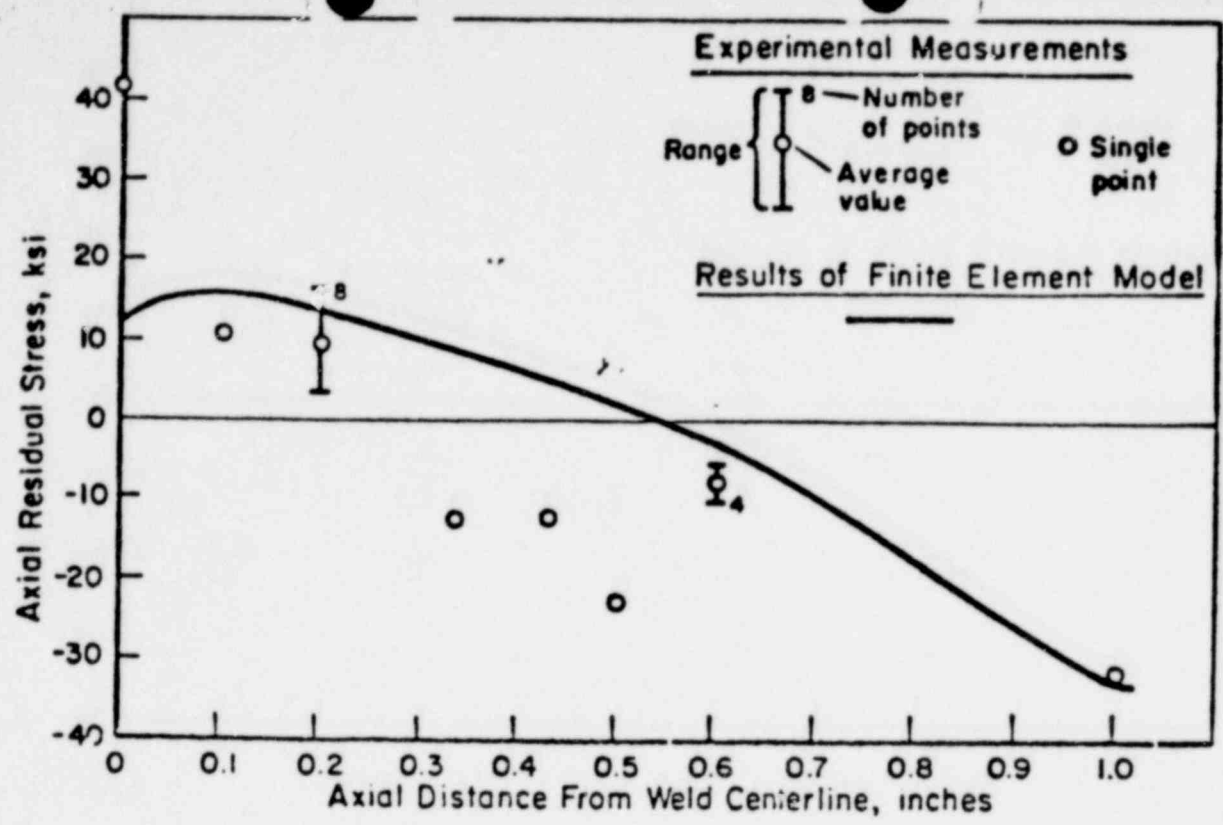


FIGURE 17. COMPARISON OF CALCULATED AND EXPERIMENTALLY DETERMINED RESIDUAL STRESSES FOR THE INNER SURFACE OF THIRTY-PASS GE EXPERIMENT

Description of the Weld Repair

The weld repair of interest was done on the HSST intermediate vessel V-8. The same weld repair procedure was applied to a two foot long prolongation cylinder with comparable dimensions to the cylindrical section of the vessel. The dimension of the weld cavity and the cylindrical section of the pipe are shown in Figure 18. The vessel material is ASTM A533, Grade B class 1 carbon steel. The size of each weld bead is about .1 inch by .1 inch. Thus, it is estimated that close to 1000 weld passes were required to fill the weld cavity.

Results of Residual Stress Model

The residual stress data for this weld repair was available along a line around the circumference of the cylindrical section of the vessel. The model is not three dimensional and cannot represent the three-dimensional aspects of the weld cavity geometry. A model was selected to represent a section of the vessel in the hoop direction through the center of the weld cavity. Another approximation in the model concerns modeling the large number of weld passes. The total number of filler passes were modeled as a single deposit of material. Because of these approximations in the model, quantitatively accurate results were not expected. However, qualitative comparisons with the data should be attainable because the model does include some aspects of the geometry and the material properties. Figure 19 shows the comparison of results obtained by computations with the model and residual stress data obtained at Oak Ridge National Laboratory. The model exhibits good agreement with the hoop stress data as shown by comparing the solid and dotted lines. Hoop and axial stress distributions from the model are on the outer surface of the vessel. The Oak Ridge data were obtained on the outer surface and from points just below the outer surface. Axial stress data is shown at one location and is also in agreement with the results of the analysis. These comparisons are very encouraging and suggest that the model can be a useful tool for residual stresses in weld repair.

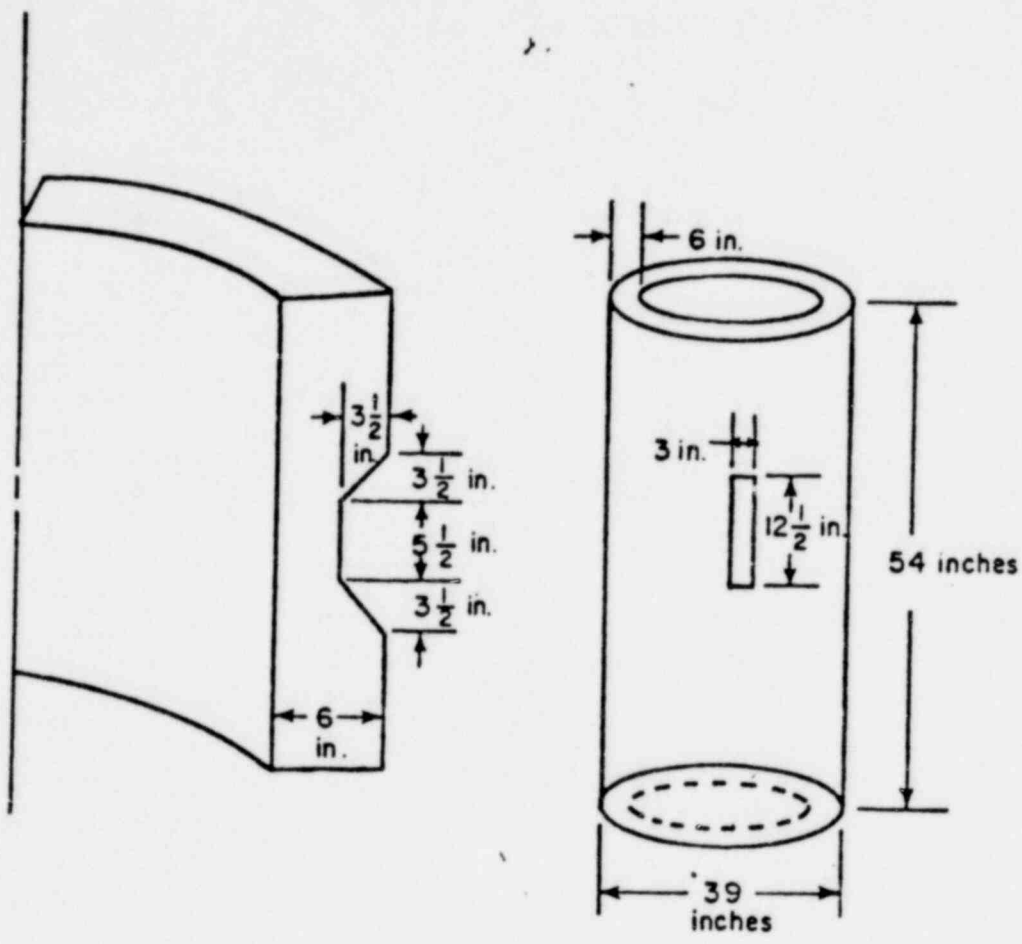


FIGURE 18. ILLUSTRATION OF WELD REPAIR CAVITY IN CYLINDRICAL SECTION OF HSST INTERMEDIATE VESSEL V-8

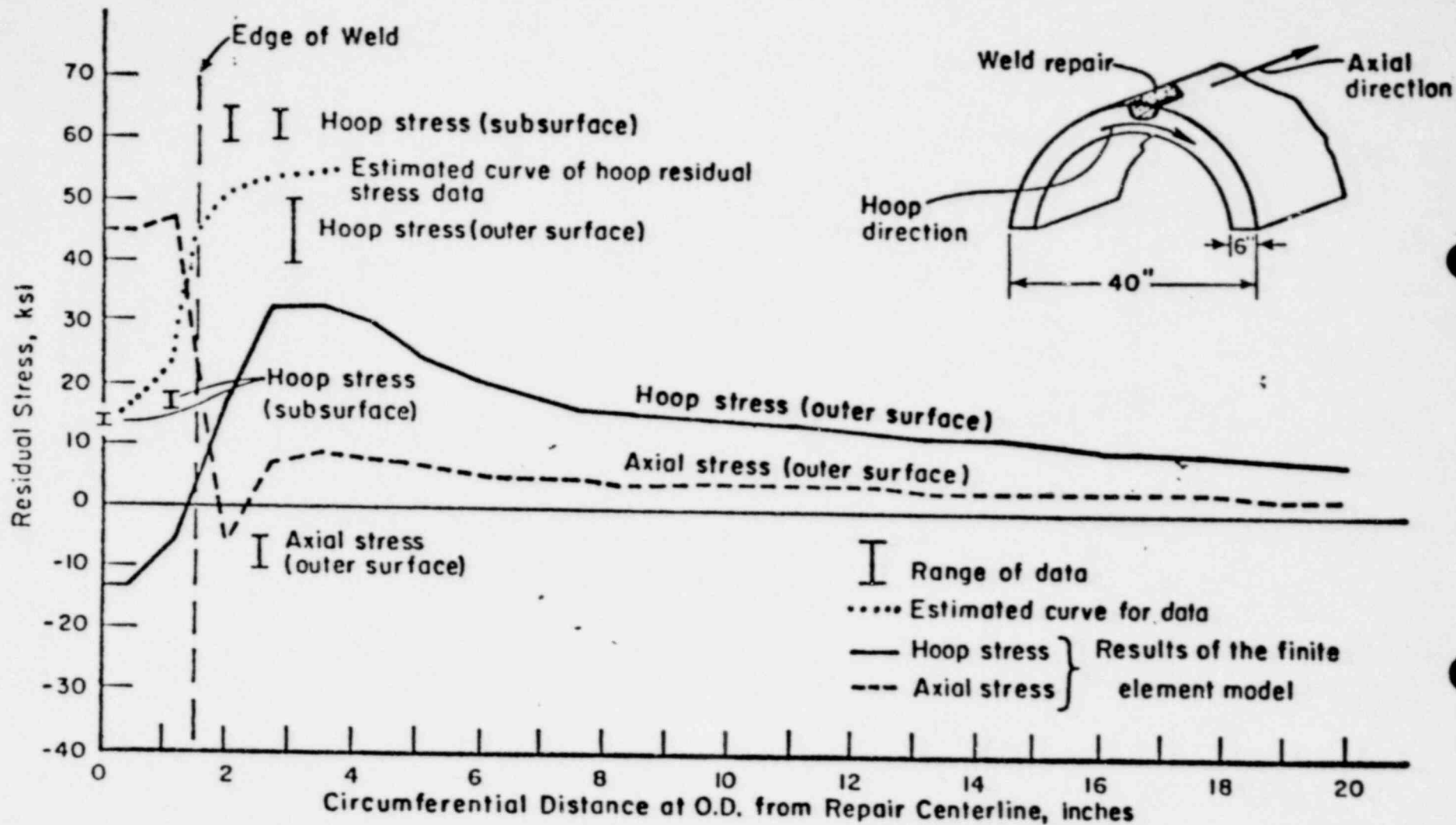


FIGURE 19. COMPARISON OF RESIDUAL STRESS DATA FOR WELD REPAIR OF HSST INTERMEDIATE VESSEL V-8 AND PRELIMINARY COMPUTATIONS BASED ON RESIDUAL STRESS MODEL

CONCLUSIONS

The residual stress and deformation model is based on a temperature model and a finite element analysis model. The model includes elastic-plastic temperature dependent material behavior for the weld and the pipe, elastic unloading from an elastic-plastic stress state, the effect of geometry changes due to welded distortions, the number and size of weld passes and the parameters included in the temperature analysis. Good comparisons between experimentally obtained residual stress data and computed values from the finite element model were obtained for the two pipes welded during the program and for two pipes reported in the literature. The number of weld passes in these pipes ranged from two to thirty. A comparison of residual stress data and preliminary results obtained for a weld repair of the HSST-Intermediate Pressure Vessel (ITV-8) indicate the model can, with modifications, be applied to studying weld repairs.

It is noted that the residual stress data were not all obtained in the same manner. The Battelle data was obtained by a chip removal procedure. The Argonne and General Electric data were obtained by removing sections of the weldment, and the Oak Ridge data was obtained by a hole drilling technique. Thus, the model results compared well with various types of residual stress measuring techniques.

Based on the results of this study it is concluded that

- A mathematical model was developed to predict the magnitude and direction of residual stresses in girth-butt welds.
- The model has been verified for pipe welds varying from 2 to 30 passes. A total of four pipes were used in the verification.
- The model predicted residual deformations that were in excellent agreement with data taken from a welded pipe.
- The model for the pipes is axisymmetric and does not contain circumferential variations of residual stress. However, the model for the weld repair does contain circumferential variations in the residual stresses.

- The accuracy of the model is due to the representation of the complex nature of the welding process. Hence, the program is of equal complexity and sophistication.
- The model has been verified for the welds described in this enclosure to the Research Information letter. Further studies are needed before it can be verified for other geometries or weld types.

BIBLIOGRAPHY AND REFERENCES

- 1 Myers, P. S. Uyehara, D. A., and Borman, G. L., "Fundamentals of Heat Flow in Welding", Welding Research Council Bulletin No. 123, July 1967.
- 2 Masubuchi, K., "Control of Distortion and Shrinkage in Welding", Welding Research Council Bulletin No. 149, April 1970.
- 3 Adams, C. M., "Cooling Rates and Peak Temperatures in Fusion Welding", Welding Journal Research Supplement, May 1958, pp 210-215.
- 4 Jhaveri, P., Moffatt, W. G., Adams, C. M., "The Effect of Plate Thickness and Radiation on Heat Flow in Welding and Cutting", Welding Journal Research Supplement, January 1962, pp 12-16.
- 5 Paley, Z., Lynch, L., Adams, C., "Heat Flow in Welding Heavy Steel Plate", Welding Journal Research Supplement, February 1964, pp 71-79.
- 6 Paley, Z. and Hibbert, P., "Computation of Temperatures in Actual Weld Designs", Welding Journal Research Supplement, November 1975, pp 385-392.
- 7 Tall, L., "Residual Stresses in Welded Plates - A Theoretical Study", Welding Journal Research Supplement, January 1964, pp 10-23.
- 8 Rodgers, D. E. and Fletcher, P. R., "The Determination of Internal Stresses from the Temperature History of a Butt Welded Pipe", Welding Journal Research Supplement, 1938, pp 4-7.
- 9 Masubuchi, K., Simmons, F. B., and Monroe, R. E., "Analysis of Thermal Stresses and Metal Movement During Welding", Battelle Memorial Institute, RSIC-820, Redstone Scientific Information Center, NACA-TM-X-61300, N68-37857, July 1968.
- 10 Gatovskii, K., "Determination of Welding Stresses and Strains with Allowance for Structural Transformations of the Metal", Svar. Proiz., No. 11, 1923, pp 3-6.
- 11 Makhnenko, V., Shekera, V., and Izbenko, L., "Special Features of the Distribution of Stresses and Strains Caused by Making Circumferential Welds in Cylindrical Shells", Avt. Svarka., No. 12, 1970, pp 43-47.
- 12 Tall, L., "Residual Stresses in Welded Plates - A Theoretical Study", Welding Journal Research Supplement, January 1964, pp 10-23.
- 13 Vaidyanathan, S., Todaro, A. F., and Finne, I., "Residual Stresses Due to Circumferential Welds", Trans. ASME, Journal of Engineering Materials and Technology, October 1973, pp 233-237.
- 14 Paley, Z., Lynch, L., and Adams, C., "Heat Flow in Welding Heavy Steel Plate", Welding Journal Research Supplement, February 1964, pp 71-79.

- 15 Wilson, E., Nickell, R., "Application of the Finite Element Analysis to Heat Condition Problems", Nuclear Engineering and Design, No. 4, 1966, pp 276-286.
- 16 Sagalevich, V. and Mezentseva, S., "Calculation of Strains and Stresses in Circular Welds", Svar. Proiz., No. 9, 1974, pp 7-10.
- 17 Kamichika, R., Yada, T., and Okamoto, A., "International Stresses in Thick Plates Weld-Overlaid with Austenitic Stainless Steel (Report 2)", Transactions of the Japan Welding Society, Vol. 5, No. 1, April 1974.
- 18 Hibbitt, H. and Marcal, P., "A Numerical Thermo-Mechanical Model for the Welding and Subsequent Loading of a Fabricated Structure", Contract No. N00014-67-A-D191-0006, Brown University, 1972.
- 19 Nickel, R., Ribbitt, H., "Thermal and Mechanical Analysis of Welded Structures", Nuclear Engineering and Design, No. 32, 1975, pp 110-120.
- 20 Friedman, E., "Thermomechanical Analysis of the Welding Process Using the Finite Element Method", Journal of Pressure Vessel Technology, August 1975, pp 206-213.
- 21 Iwamura, Y. and Rybicki, E. F., "A Transient Elastic-Plastic Thermal Stress Analysis of Flame Forming", ASME Trans. Journal of Engineering for Industry, February 1973.
- 22 Rybicki, E. F., Ghadiali, N. D., and Schmueser, D. W., "An Analytical Technique for Evaluating Deformations due to Welding", Paper Submitted to ASME WAM, November 27, December 2, 1977, held in Atlanta, Ga.
- 23 Rosenthal, D., "Mathematical Theory of Heat Distribution During Welding and Cutting", Welding Journal Research Supplement, May 1941, pp 220-234.
- 24 Cheng, C. F., Ellingson, W. L., Kupperman, D. S., Park, J. Y., Poeppel, R. B., and Reiman, K. J., "Corrosion Studies of Nuclear Piping in BWR Environments", Quarterly Report, Argonne National Laboratories, June, 1976.
- 25 "Studies on AISI Types -304, -304L, and -347 Stainless Steels for BWR Applications", NEDO-20985-1, September, 1975.
- 26 Klepzer, H., et al., "Investigation of Cause of Cracking in Austenitic Stainless Steel Piping", General Electric Report No. NEDO-21000-1, July, 1975.

14-111

1568 169

782190294